

P1.14 NONLINEAR SCALE INTERACTIONS IN LAKE-EFFECT CLOUDS

Natasha L. Miles* and Johannes Verlinde

Department of Meteorology, The Pennsylvania State University, University Park, Pennsylvania 16802

1. INTRODUCTION

Although horizontal roll vortices have been studied for decades, the atmospheric conditions required for roll development are still being debated in the literature. Rolls are most often observed in cases of moderate positive surface buoyancy flux and high shear (e.g., Weckwerth et al. 1997), and these are the conditions for which most models predict rolls (e.g., Glendening 2000). There have, however, been roll observations in other atmospheric conditions (e.g., Kelly 1984; Kristovich 1993).

The present study examines convective organization in a lake-effect event over Lake Michigan that, instead of having a single dominant organization, switches between marginally linear organization and more random cellular organization. The atmospheric conditions during this lake-effect event are not typical for roll development—the surface buoyancy flux is very large and the shear is only moderate. In this study we explore the possibility that nonlinear scale interactions are a large enough source to the roll turbulence kinetic energy (TKE) to play a significant role in the observed mode switching.

2. TRANSIENT LINEAR ORGANIZATION

A. WSR-88D

The data for this study were measured during the Lake-Induced Convection Experiment (Lake-ICE) which was conducted in the Lake Michigan area. Kristovich et al. (2000) describe the coordinated efforts and overall setup of Lake-ICE. In the current study we focus on results from 13-14 January 1998 at the downwind shore. During the analysis period, the average cloud base height is 630 m and the average cloud top height is 890 m. The average in-cloud wind speed is 7.5 m s^{-1} and the average wind direction is 300° . The average temperature difference between the lake and the surface air is 14°C .

An example of the National Weather Service Weather Surveillance Radar-1988 Doppler (WSR-88D) radar reflectivity field during the analysis period is shown in Fig. 1. This example is from a relatively linearly organized period. The center of the image is 16 km west of Muskegon, MI. Throughout the analysis period, the images depict a transition from relatively organized linear convection to more cellular, disorganized convection, and back to marginally linear organization within a 5-hour

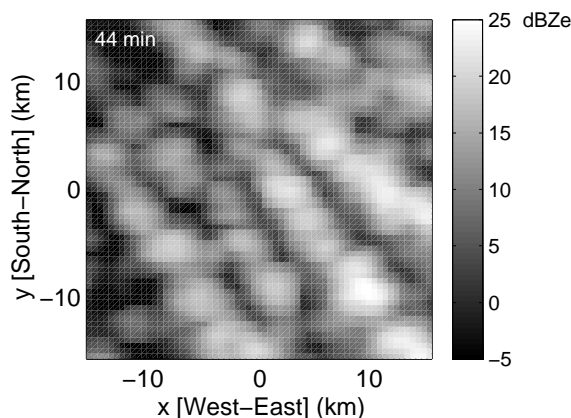


Figure 1: Example of WSR-88D reflectivity field from a relatively linearly organized period.

time frame. Auto-correlation analysis of the images (not shown) also indicate that the organization of the system switched between roughly linear and predominantly cellular, never quite reaching a well-organized state. In Fig. 1 the size of the reflectivity cells is 3-5 km. The time-averaged roll wavelength is $6.3 \text{ km} \pm 0.8 \text{ km}$.

B. PSU cloud radar

The primary data for this study are air vertical velocities obtained using The Pennsylvania State University (PSU) cloud radar. This study is unique in its long duration of continuous high resolution vertical velocity data. Eighteen hours of 94-GHz Doppler cloud radar vertical velocity data, available every 7.5 s at around eight in-cloud heights, were measured on the downwind (eastern) shore of southern Lake Michigan in Muskegon, MI. Operating at a higher frequency than a typical weather radar, the cloud radar is sensitive to small cloud droplets, as well as larger drops. The cloud radar data are processed to obtain Doppler spectra (reflectivity as a function of vertical velocity) and filtered through a cloud mask (Clothiaux et al. 1995).

Each Doppler spectrum is the quiet-air fall velocity spectrum of the cloud particles broadened by turbulent motions within the radar resolution volume and shifted by the mean vertical velocity in the radar resolution volume. We use the deconvolution technique developed by Babb et al. (2000) to remove the turbulent broadening effects. We assume the smallest droplets detected

*Corresponding author address: Natasha L. Miles, Dept. of Meteorology, 503 Walker Building, University Park, PA 16802; E-mail: nmiles@essc.psu.edu

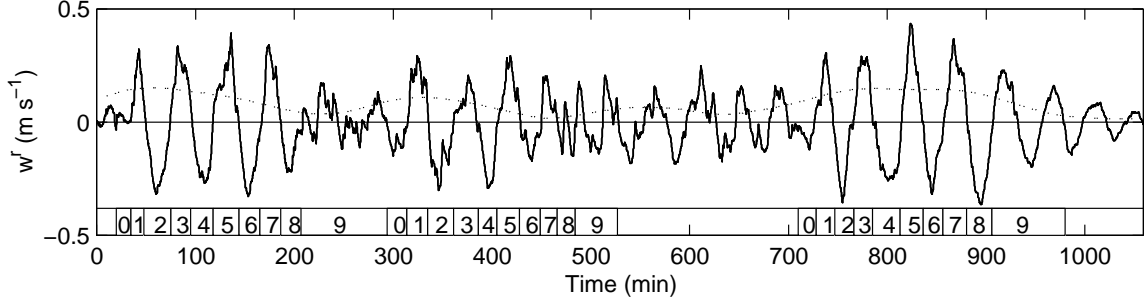


Figure 2: Roll-scale vertical velocity at a height of 720 m (solid line) and roll-scale wavelet amplitude (dotted line). Stages 0-9 of the three roll life cycles are indicated near the bottom.

by the radar are tracers of the wind, having negligible fall velocity. Then the mean vertical velocity in the radar resolution volume is simply the shift of the Doppler spectrum along the velocity axis. For the present study we are interested in only the air motions, not the particle fall velocities.

C. Wavelet Analysis

Multiple scales of motion are commonly observed in cases of boundary layer rolls, as in many other atmospheric phenomena. To study the interaction between these scales, the variability in time of the power in frequency bands is crucial. Wavelet analysis is a way to extract both frequency and time information. Using the method described by Torrence and Compo (1998), wavelet power spectra are calculated for the vertical velocity time series at several in-cloud heights. Although the power changes with time, several dominant scales are found in the time series as a whole:

(i) Turbulence scale (< 8.3 min): The turbulence scale, as defined for the purposes of this paper, includes scales the size of individual thermals down to the smallest time scales detectable in the data set. Using the time-averaged in-cloud horizontal velocity of 7.5 m s^{-1} as an estimate and Taylor’s frozen atmosphere hypothesis, the approximate sizes included in the turbulence scale are 100 m - 3.7 km. The scale corresponding to the typical 1.5 aspect ratio found in turbulence spectra (Kaimal et al. 1976) is within this range. Our “turbulence scale” contains part of the energy-containing range and the inertial subrange.

(ii) Core scale (8.3-16.5 min): Using the average in-cloud wind speed of 7.5 m s^{-1} , the sizes included in the core-scale period range are 3.7-7.4 km, roughly in agreement with the range of reflectivity cell sizes observed in the WSR-88D images (Fig. 1).

(iii) Roll scale (39.3-55.6 min): The average roll wavelength determined from the WSR-88D analysis is 6.3 km. The difference in advection speeds between the rolls and cores allows the separation between the two in frequency even though they are of similar spatial size.

The contributions to the vertical velocity due to the different physical structures are separated by highpass

and bandpass filtering the data, using the cutoff periods suggested by the wavelet analysis. In Fig. 2, the roll-scale (bandpass-filtered) vertical velocity (w_r) and the wavelet amplitude integrated through the roll period range are shown. There are four cycles apparent in the roll-scale vertical velocity, corresponding to the four peaks in the roll-scale range from wavelet analysis. The third cycle is, however, comparatively very weak.

D. Composites

Compositing is a way to isolate systematic from unsystematic variations. We composite, or average, over the three well-defined cycles. Each cycle is partitioned into ten stages. The stages are defined such that roll updrafts occur during odd-numbered stages and roll downdrafts occur during even-numbered stages. Stages 0-1 are prior to the maximum roll intensity, and stage 5 is a mature roll stage. For each of the cycles excluding the last, the rolls have decayed by stage 8.

We calculate the variance in each of the scales, averaged over the cloud depth. Shown in Fig. 3 is the turbulence- and roll-scale TKE, plotted as a function of stage. The core-scale TKE (not shown) is strongly correlated to the turbulence-scale TKE, with a correlation coefficient of 0.97. The results are normalized by the average of the TKE in all ten stages for each scale. The normalization factor for the roll-scale TKE is about 4% of that of the turbulence-scale TKE. The error bars are calculated as the standard deviation of the cycles.

In Fig. 3, in which successive downdraft and updraft stages are grouped together, the overall trend of the roll life cycle is very little variance at stage 0-1, maximum variance during the mid-range stages, and by stages 8-9 the variance has decreased to below the mean. This behavior is a consequence of the definition of the stages. The turbulence-scale variance peaks at stages 0-1, prior to the peak in the roll-scale variance. The turbulence-scale variance then falls off, and begins to increase over the latter stages. These results imply a possible exchange of energy between turbulence and roll scales.

3. POSSIBLE CAUSES

We will now consider possible causes for the observed

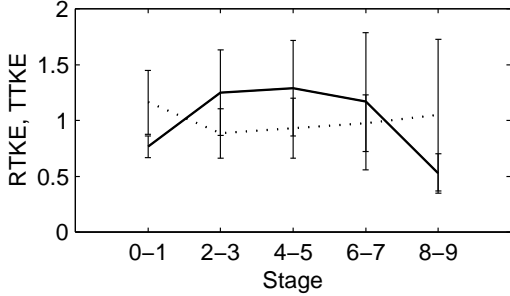


Figure 3: Composite of normalized integrated roll-scale variance (solid line) and turbulence-scale variance (dotted line) as a function of stage in the roll life cycle.

mode switches. Glendening (2000) and LeMone (1976) considered roll TKE budgets, including nonlinear interaction terms. The terms in the roll-scale TKE equation are the local time rate of change of the roll-scale TKE, advection, mean shear production, buoyancy production, pressure transport, Coriolis, and the interscale transfer and turbulent transport terms. Unfortunately, a detailed budget analysis is not possible for this study. Data to supplement the high temporal resolution vertical velocity profiles retrieved from cloud radar measurements are either too infrequent, separated spatially, or not available. We can, however, discuss the two most important production terms for roll TKE: buoyancy in terms of the bulk parameterizations of the surface measurements and the shear from wind profiler measurements.

It is likely that many factors contribute to the observed mode-switching—from cellular to linear to cellular organization. Previous work suggests that the amount of boundary layer shear or low-level shear may be a trigger between the different modes. Although shear may contribute, it is not the primary cause of the mode-switching in this case, as indicated by comparing the time series of shear (not shown) with the time series of roll-scale wavelet amplitude. The surface buoyancy flux (not shown) decreases linearly throughout the analysis period and is not correlated with the organization. The ratio of the friction velocity to the convective velocity scale (u_* / w_*) is significantly less than the critical value (0.35; Sykes and Henn 1989) throughout the entire analysis period. The largest value of u_* / w_* is about 0.2 and occurs near the beginning of the analysis period.

Profiles of turbulence-scale vertical velocity variance (not shown) reveal consistent maxima during stages 0-1 (prior to the maximum roll TKE) and during stages 7-8 (after the maximum roll TKE). The variance profiles in other stages are, for the most part, either decreasing with height or constant with height. The unfiltered vertical velocity (not shown) has a maximum at stage 1 and a secondary maximum at stage 7. The additional latent heating associated with the maxima in the vertical velocity contributes to in-cloud buoyancy, which, in turn, produces primarily turbulence-scale, flow-filling

TKE. The changes in the variance profiles again suggest the possibility of scale interactions.

A. Nonlinear scale interactions

From the cloud radar vertical velocity, we calculate the vertical transport and interscale transfer terms involving only the vertical velocity. Of these terms, there are five containing only the vertical velocity for the vertical roll TKE equation. The two terms that are significant in this case are the vertical transport of turbulence-scale TKE by the rolls $[-\partial(\overline{w^r w^t w^t})/\partial z]$ and roll shear stress interscale transfer $[\overline{w^t w^t \partial w^r}/\partial z]$. Following Glendening (2000), we call these terms stress work and roll shear stress, respectively.

The stress work term (not shown) is generally positive during roll updrafts and negative during roll downdrafts, but the magnitude is larger during the updraft stages, indicating that, overall, it is a gain in the roll TKE equation. When the stress work term is positive, turbulence-scale stress is transported into the cloud layer by the rolls and “consumed” by the roll-scale TKE. The roll shear stress interscale transfer term (not shown) counteracts the stress work term, being negative in roll updraft stages and positive in roll downdraft stages. The negative roll shear stress terms indicate downscale transfer from the roll scale to the turbulence scales, whereas positive values indicate upscale transfer.

We integrate the the sum of the two dominant roll-turbulence nonlinear interaction terms over the cloud layer to determine the net effect of the interactions (Fig. 4). Nonlinear interactions of the roll and turbulence scales are a source to roll TKE during the middle of the roll life cycle, strengthening the rolls. We estimate the characteristic time scale of the nonlinear interactions (by dividing the magnitude of the roll-scale TKE during stages 4-5 by the net nonlinear interaction term during stages 4-5) to be about 4 min. We note that without residual roll-scale variance from previous cycles the nonlinear interaction terms vanish since all the terms contain w^r . Thus nonlinear interactions cannot instigate roll-scale TKE when there is none. Although the transient rolls observed during this study occurred in atmospheric conditions not normally considered favorable for rolls, it is possible that the conditions were more favorable prior to the observations. Even when the conditions ceased to be favorable, rolls continued to exist transiently, due to, at least in part, nonlinear interactions.

All of the turbulence transport terms, including stress work, must individually sum to zero over the depth of the boundary layer, assuming no transport to the free atmosphere. When the stress work term, integrated over the cloud layer, is positive, it must be negative in the subcloud layer. While stress work acts to strengthen the rolls in the cloud layer (where we observe the changes in roll organization with cloud radar and WSR-88D radar), the roll motion must be correspondingly less organized in the subcloud layer.

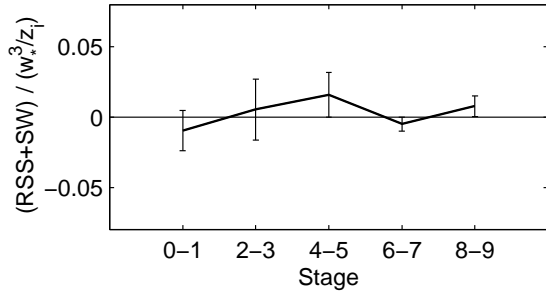


Figure 4: Composite of the sum of stress work (SW) and roll shear stress (RSS), normalized by w_*^3/z_i , and integrated over the cloud layer, as a function of stage in the roll life cycle.

B. Possible Scenario

A possible scenario for the mode switching is the following. The mean vertical velocity is highest prior to roll strengthening and has a smaller maxima just before roll decay. Since mean vertical velocity is typically found to be correlated with liquid water content, the increase may be associated with additional latent heating, providing TKE to the turbulence-scale eddies. In agreement with this scenario, we observe in-cloud turbulence-scale vertical velocity variance peaks both prior to and after the maximum roll strengthening. The two dominant nonlinear interaction terms for the roll-scale TKE are the vertical transport of turbulence-scale TKE by the rolls (stress work) and roll shear stress interscale transfer. Since the sum of these terms is proportional to the gradient of the turbulence-scale variance, the in-cloud net nonlinear interaction term (integrated over the depth of the boundary layer) is minimized when an in-cloud turbulence-scale vertical velocity variance peak is observed and maximized when the in-cloud turbulence-scale vertical velocity variance decreases with height. Consequently the nonlinear interaction terms are a source to the rolls in the middle stages of the roll life cycle observed in this case.

4. SUMMARY

There are discrepancies in the literature as to the atmospheric conditions required for roll formation. The present lake-effect event, with large positive buoyancy flux and only moderate shear, is not within the range of buoyancy parameters most often associated with rolls. Neither is the low-level shear, nor the mean boundary layer shear, found to drive the organizational mode switching. Changes in the surface buoyancy flux are also not correlated to the changes in organization. There is, however, evidence that nonlinear interactions between the roll-scale vertical velocity and the turbulence-scale vertical velocity acted to strengthen the rolls.

The duration of measurements is critical to observations of the mode switching, which occurred, in this case, on the time scale of about five hours. While there are

a few observations of mode switching (e.g., Kristovich et al. 1999), a likely cause for the scarcity is the duration of continuous measurements required. This study highlights the danger of observing rolls and the associated conditions for a short time compared to the mode-switching frequency and making conclusions about the conditions necessary to form rolls. This result may explain, in part, the discrepancy between the ranges of atmospheric conditions in which rolls are observed—the data sets may not have been long enough to capture the essential physics, especially for marginal cases.

While we have focussed on a Eulerian description of the observed changes in convective organization, a Lagrangian perspective may be necessary to fully understand the phenomenon. Changes in organization and variance profiles may not be caused locally, instead being delayed by the advection time from the source region. The combination of increasing boundary layer depth, increasing wind speed, and decreasing temperature difference across the lake leads to the conditions being favorable for rolls on the upwind shore, unfavorable over the middle of the lake, and recovering by the downwind shore.

The processes by which heat and moisture are transferred from warm water surfaces to the comparatively cold atmosphere occur over a wide range of spatial scales. Roll-scale circulations significantly modify the environment of the smaller-scale turbulence phenomena. Likewise, turbulence-scale eddies are the intermediate agents between the enhanced surface fluxes and the intensification of the roll-scale circulations. Much is still not understood about these important processes, and still less is known about interactions between processes on each of these scales. An understanding of how these processes work in conjunction to link the surface to roll-scale flows is necessary if we are to develop more accurate models of large-scale storm development.

Acknowledgments. We gratefully acknowledge the help of J. Wyngaard. Wavelet analysis software was provided by C. Torrence and G. Compo, and is available at <http://paos.colorado.edu/research/wavelets/>. The deconvolution code was supplied by D. Babb. This work was supported by the National Science Foundation (under grants ATM-9629343 and ATM-9596107).

REFERENCES

- Babb et al., 2000, *JAOT*, **17**, 1583–1595.
- Clothiaux et al., 1995, *JAOT*, **12**, 201–229.
- Glendening, 2000, *JAS*, **57**, 2297–2318.
- Kaimal et al., 1976, *JAS*, **33**, 2152–2169.
- Kelly, 1984, *JAS*, **41**, 1816–1826.
- Kristovich, 1993, *BLM*, **63**, 293–315.
- Kristovich et al., 1999, *MWR*, **127**, 2895–2909.
- Kristovich et al., 2000, *BAMS*, **81**, 519–542.
- LeMone, 1976, *JAS*, **33**, 1308–1320.
- Sykes and Henn, 1989, *JAS*, **46**, 1106–1118.
- Torrence and Compo, 1998, *BAMS*, **79**, 61–78.
- Weckwerth et al., 1997, *MWR*, **125**, 505–526.